JAEA-Review
2014-016

JAEA-Review

Literature Review on Experiments and Models Associated with Degradation and Oxidation of Boron Carbide Control Material during Severe Accidents

Xiaoyu ZHENG, Jun ISHIKAWA, Hiroto ITOH
Hitoshi TAMAKI and Yu MARUYAMA

Risk Analysis and Application Research Unit
Nuclear Safety Research Center

June 2014

Japan Atomic Energy Agency
日本原子力研究開発機構

独立行政法人日本原子力研究開発機構　研究技術情報部　研究技術情報課
〒319-1195　茨城県那珂郡東海村白方白根2番地4
電話 029-282-6387, Fax 029-282-5920, E-mail:ird-support@jaea.go.jp

Intellectual Resources Section, Intellectual Resources Department,
Japan Atomic Energy Agency.
2-4 Shirakata Shirane, Tokai-mura, Naka-gun, Ibaraki-ken 319-1195 Japan
Tel +81-29-282-6387, Fax +81-29-282-5920, E-mail:ird-support@jaea.go.jp

JAEA-Review 2014-016

Literature Review on Experiments and Models Associated with Degradation and Oxidation of Boron Carbide Control Material during Severe Accidents

Xiaoyu ZHENG※1, Jun ISHIKAWA, Hiroto ITOH※2, Hitoshi TAMAKI and Yu MARUYAMA

Risk Analysis and Application Research Unit
Nuclear Safety Research Center
Japan Atomic Energy Agency
Toukai-mura, Naka-gun, Ibaraki-ken

(Received March 6, 2014)

Boron carbide (B_4C) is one kind of neutron absorbing control rod/blade materials used in light water reactors (LWRs). In the Fukushima Daiichi nuclear power station (NPS), all units used B_4C as absorber material. The degradation of control rod/blade will affect the early phase of in-vessel core melt progression. Furthermore, the release of carbon compound gases including carbon dioxide (CO_2) as well as boron compounds due to the oxidation of B_4C with steam is possible to affect source terms of radioactive materials. Past experiments related to B_4C degradation and oxidation and numerical modeling in severe accidents codes are investigated in the current report with a main view to apply the acquired knowledge into the modification of THALES-2 developed at JAEA as an integral severe accident analysis code. The eutectic interactions of B_4C with other materials such as stainless steel and Zircaloy will lower the melting point of control rod/blade. The Nagase's correlations for eutectic interaction are selected as one of candidates to be applied into THALES-2. The oxidation reaction of B_4C with steam will release considerable amount of thermal energy, and form CO_2, boric acids and boron oxide, which could make an impact onto source terms by changing the pH value of a water pool where those dissolve. The correlation determined by Institut de Radioprotection et de Sûreté Nucléaire (Radiation and Nuclear Safety Institute, IRSN) is chosen to be used in the modeling of oxidation reaction in THLAES-2.

Keywords: Boron Carbide, Light Water Reactor, Severe Accident Codes, Eutectic Interaction, Oxidation, Reaction Rate

---

※1 Post-Doctoral Fellow

※2 Collaborating Engineer

JAEA-Review 2014-016

シビアアクシデント時における炭化ホウ素制御材の損傷及び酸化に係わる実験及びモデルに関する文献調査

日本原子力研究開発機構　安全研究センター
リスク評価研究ユニット

鄭　嘯宇[※1]・石川　淳・伊藤　裕人[※2]・玉置　等史・丸山　結

（2014 年 3 月 6 日　受理）

炭化ホウ素（B_4C）は軽水炉における制御材の一つであり、福島第一原子力発電所では全号機において用いられている。B_4C 制御棒／ブレードの損傷は、原子炉容器内における早期の炉心溶融に影響する。また、B_4C の水蒸気酸化による二酸化炭素（CO_2）を含む炭素化合物やホウ素化合物の発生は、放射性物質のソースタームに影響を及ぼす可能性がある。本報告書では、原子力機構において整備しているシビアアクシデント総合解析コード THALES-2 の高度化を視野に入れて、B_4C の損傷及び酸化に係わる既往の実験及びモデル化について文献調査を行なった。制御棒／ブレードの溶融温度は B_4C とステンレス鋼やジルカロイとの共晶反応により低下する。既存の共晶モデルを検討し、Nagase らのモデルを THALES-2 に組み込むモデルの一つとして選定した。また、B_4C と水蒸気との酸化反応により大量の熱が放出されるとともに、CO_2 やホウ酸、酸化ホウ素が生成され、それらが溶解することにより、ソースタームに影響を与える水相の pH 値が変化し得る。B_4C の水蒸気酸化については、フランス放射線防護原子力安全研究所（IRSN）が開発した酸化反応速度モデルを THALES-2 に導入するモデルの候補として選定した。

原子力科学研究所（駐在）：〒319-1195　茨城県那珂郡東海村白方白根 2-4
※1　博士研究員
※2　技術開発協力員

Contents

目次

1 Introduction

Boron carbide (B_4C) is used as neutron absorbing material in many light water reactors (LWRs) worldwide, e.g. boiling water reactors (BWRs), Russian VVERs, French pressurized water reactors (PWRs) and Areva-designed EPR [1]. The B_4C is filled in stainless steel (SS) claddings which are inserted into Zircaloy-4 guide tubes for a PWR or inserted into gaps among fuel assemblies for a BWR. Some PWR designs use B_4C-pellets possibly together with metallic Ag-In-Cd absorber alloy in one control rod, which is called hybrid control rod. This PWR configuration is characteristic for the 1300 MWe FRAMATOME reactors and for the Westinghouse VVANTAGE6 core, recently designed for Temelin NPP VVER-1000. It should be mentioned that the original design of VVER-1000 uses B_4C-powder and SS guide tubes [2].

Under severe accident conditions, the oxidation of B_4C may contribute to the production of both hydrogen and other gases such as CO, CO_2, and large amounts of B-compound aerosols. The B_4C is also found to favor the core liquefaction during the bundle degradation experiments such as CODEX- B_4C, QUENCH-07 [3]. Most importantly, B_4C is applied in all units of the Fukushima Dai-ichi nuclear power plant. According to state-of-the-art research, the complete failure of the absorber blades probably happened in the rather early phase of the accident [4]. Two topics are out of the scope of this report: the potential formation of methane CH_4 which has been proven as insignificant as negligible in many publications, and the recriticality of reactor after the reflooding of degraded core with unborated water.

This report aims at clarifying the following questions based on worldwide experiments and severe accident codes.

- What is the impact of B_4C on core degradation?
- What knowledge has already been confirmed for B_4C control rod degradation?
- How to determine models of B_4C/SS and B_4C/Zircaloy eutectic interactions? At what temperature eutectic interactions happen?
- How to determine correlations of pure B_4C pellet or powder oxidation and B_4C-bearing melt oxidation? At what temperature and under what conditions, B_4C-oxidation happens?
- How much uncertainties are caused by the B_4C oxidation process in the evaluation of hydrogen and radioactive source terms?

2 Literature Review

Two aspects will affect the behavior of control rod in the process of core degradation: (1) eutectic interaction between B_4C and other materials; (2) oxidation of pure B_4C pellet or powder and B_4C/SS mixture. Previous research has been started from the end of 1980s and a great amount of knowledge has been gained from experiments (both separate effect tests and integral tests) and mathematical analyses during 1990s and 2000s.

2.1 Eutectic interaction

Under ideal mechanical and atmospheric conditions, eutectic interactions between core components can result in the formation of liquid layers at relatively low temperatures (far below the melting point of a pure material). Experiments by Hofmann and Uetsuka show that at 1250 ºC, SS tube (thickness: 1 mm) can be converted by B_4C into a liquid phase within 100 seconds, and at 1200 ºC a Zircaloy-4 layer (thickness: 0.5 mm) can be consumed by SS within 10 seconds [2].

Hofmann et al. [5] studied the chemical behavior of B_4C absorber material with stainless steel and Zircaloy-4 in the temperature 800 – 1600 ºC. Reaction kinetics can be described by parabolic rate laws. The compatibility specimens were quickly and completely liquefied at about 1250 ºC for the B_4C/SS reaction couples and at about 1650 ºC for the B_4C/Zircaloy-4 reaction couples, both of which proved that the liquefaction occurs below the melting points of the components. Five years later, Hofmann et al. [6] published results of Zircaloy-4 and stainless steel interactions at high temperatures. The eutectic interaction was studied in the temperature range 1000-1400 ºC. Results also showed the liquefaction of components occurs below their melting points. The existence of Zircaloy oxide delayed the eutectic interaction between SS and Zr but could not prevent it, similarly, which could be described as parabolic rate laws.

The DF-4 experiment [7] in the Annular Core Research Reactor (ACRR) at Sandia National Laboratories is the first in-pile experiment to examine the behavior of BWR fuels and control elements under severe accident conditions. Control blade failed in DF-4 experiment when temperature reached between 1247 ºC and 1297 ºC. The effective melting point of the stainless steel was believed to have been lowered due to an interaction between Fe and B_4C, which was also found by Hofmann et al. [5]

Sepold et al. [8] summarized results of CORA-16 (1988), CORA-17 (1989), and CORA-18 (1990) experiments. Results showed that the presence of B_4C caused the formation of a “low-temperature” melt at around 1250 ºC. The liquefaction was due to an interaction between B_4C and steel.

Uetsuka et al. [9] introduced experiments conducted at JAERI (currently JAEA) about investigation on eutectic interactions for various binary systems of core component materials including B_4C/SS (from 800 ºC to 1350 ºC) and B_4C/Zircaloy-4 (from 900 ºC to 1700 ºC). It was found that the reaction generally obeyed a parabolic rate law. Later, Nagase et al. [10, 11] at JAERI published detailed experimental results. The formation of liquid phase at the reaction interface would cause an obvious discontinuity in the temperature dependence of the parabolic rate law constants.

Experiments were performed by Belovsky et al. [2] with the aim at verifying and improving the

B_4C/SS eutectic interaction model, which was developed for the ICARE2 code. The B_4C/SS and B_4C/SS/Zircaloy-4 specimens were exposed to argon and steam in the temperature range 800-1500 ºC. Results show that SS oxide did not represent any significant barrier for the failure of the B_4C/SS system. On the contrast, ZrO_2 scale was able to keep the B_4C/SS/Zircaloy-4 system intact up to relatively high temperatures, but the formation of ZrO_2 layer cannot avoid eutectic interactions. Parameters in the JAERI parabolic correlations were optimized by Belovsky in order to well predict the measured failure temperatures.

Based on experiments performed by Hofmann et al. [5, 6], Veshchunov et al. [12, 13] have developed mathematical models for B_4C/Zircaloy and B_4C/SS, respectively. One parabolic rate law by Arrhenius correlation was proposed for the B_4C/Zircaloy interaction, which explained qualitatively the reaction system behavior in the temperature range (from 800 ºC to 1500 ºC) up to the onset of the eutectic liquid phase formation in the reaction zone. At 1600 ºC, an abrupt jump of the reaction rate by about two orders of magnitude was observed. At $T \geq 1650$ ºC, the compatibility specimens were completely liquefied. For the B_4C/SS interaction, one theoretical model (parabolic rate law) had been developed according to experiments at temperatures of 1000 ºC, 1100 ºC and 1200 ºC. Similarly to B_4C/Zircaloy interaction, when $T \geq 1200$ ºC, a sharp bend in the Arrhenius line was discovered.

Bertrand et al. [14] qualitatively introduced that during an hypothetical severe accident transient, once the temperature of the control rod had reached approximately 800 ºC, a solid/solid B_4C/SS interaction occurs, leading to a liquefaction of the reaction zone when the temperature exceeded 1227 ºC. Once the stainless steel was totally liquefied, that was approximately near 1527 ºC, depending on the temperature transient and on the B_4C/SS amount ratio, the liquid will interact with the guide tube made of Zircaloy and thus, triggers its rupture. After that the B_4C/SS mixture relocate to lower part of the core, the oxidation of remaining B_4C would happen.

Extensive series of tests were performed by Steinbrück [15, 16] for the investigation of B_4C absorber rods degradation. Rapid melt formation due to eutectic interactions between stainless steel (cladding tube) and B_4C on the one hand and between the steel and Zircaloy-4 (guide tube) one the other hand were observed at temperatures above 1250 ºC. Complex multi-component and multi-phase melts were formed. Separate-effect tests (LAVA furnace) showed that B_4C can liquefy huge amounts of stainless steel at 200 K below its melting temperature. It is concluded that (1) 1000 ºC: no significant interactions of stainless steel, boron carbide and Zircaloy; (2) 1200 ºC: local interactions of stainless steel, boron carbide, and Zircaloy; (3) ≥ 1250 ºC: rapid, complete liquefaction of metals (steel, Zircaloy) in the gap between B_4C pellet and external ZrO_2 oxide scale; (4) ≥ 1450 ºC: failure of the oxide scale and rapid oxidation of absorber melt and remaining B_4C pellets.

de Luze et al. [17] and Barrachin et al. [18] concluded bundle degradation phenomena (early and late phase, respectively) which were observed in Phébus FP test. One test in the series used a B_4C control rod.

(1) It was summarized by de Luze et al. [17] that the stainless steel of the cladding material is thermodynamically unstable with respect to the B_4C absorber. Reaction started above the eutectic temperature of 800 ºC, but solid-solid reaction is slow so in practice liquid phases only start to

appear from 1000 ºC upwards. Rapid liquefaction occurred above 1250 ºC as a result of interaction between the steel components with boron on one hand, and with carbon on the other. The B_4C-SS melt reacted eutectically with the Zircaloy guide tube again to give Zircaloy liquefaction above 1250 ºC. As long as the guide tube was intact, the liquefied alloy composed of B_4C, SS and Zircaloy was held in place or relocates internally in the gap between the cladding and guide tube. Significant external relocation of B_4C-bearing melt occurred on failure of the oxide shell on the outside of the guide tube, which would depend on its thickness.

(2) Barrachin et al. [18] pointed out that B_4C control rods promoted bundle degradation more than those of (Ag-In-Cd) in terms of timing (earlier) and melt fluidity (increased due to B_2O_3 presence which decrease melt viscosity).

2.2 Oxidation

B_4C oxidation is very exothermic and may have a significant effect on the early phases of degradation, particularly during the reflooding. However, the complex chemistry of this reaction (production of B-compound materials and other gases) is still under investigation, so related simplified models applied in current severe accident codes are of great uncertainties. The reaction products will affect the fission product chemistry in primary system as well as containment, and generated thermal energy will affect the process of core degradation. Many small-scale and large-scale experiments have been conducted, especially since 2000. A great number of knowledge has been obtained and modeling of B_4C oxidation has been improved in severe accident codes.

Even though the research of B_4C oxidation at high temperatures started since 1980s [19-21] and simple models were developed and applied in early versions of MELCOR and SCDAP/RELAP5, a comprehensive description of modeling methodology was missing. Belovsky [22] highlighted the key points of the B_4C oxidation and performed a simple heat balance analysis of the B_4C/steam and B_4C/air chemical reactions. Until then, the B_4C oxidation phenomenon was qualitatively well described below 1000 ºC and no reliable data existed for the reaction kinetics especially above 1000 ºC. It was found that the B_4C oxidation is an exothermic reaction, releasing more heat in air than in steam. The formation of boric acids from boron oxide increased the heat release from B_4C by 10%, in the worst case.

The core loss during a severe accident (COLOSS) is a 3-year project which started in 2000. Adroguer et al. [2, 23] provided mid-term and final results of COLOSS project, respectively. Two of main topics involved in the project are: (1) oxidation of pure B_4C material; and (2) degradation-oxidation of prototypic B_4C control rods. Corresponding models were developed and implemented in severe accident computer codes (detailed ICARE/CATHARE, ATHLET-CD and SVECHA codes, and integral ASTEC and MAAP codes). Break-through was achieved on the oxidation of B_4C-metal mixtures. Separate effect tests of the B_4C oxidation and related effects were investigated mainly in FZK (Forschungszentrum Karlsruhe, now Karlsruhe Institute of Technology) using TG-tests, BOX rig and QUEHCN-SR rig and IRSN (Institut de Radioprotection et de Sûreté Nucléaire) using VERDI furnace. Three bundle tests were carried out with a central B_4C control rod: one CODEX-B_4C test with a VVER bundle and two QUENCH-07 and

QUENCH-09 tests with a PWR bundle type.

Bertrand et al. [14] modeled the degradation of a B_4C control rod during a PWR severe accident. Models applied were validated against separate effect results and against the integral Quench-09 test. The validation work showed that models were quite efficient to compute the B_4C taking into account the main overall parameters, namely, the temperature, the steam partial pressure and the total pressure. Corresponding discoveries were also applied in the pre-test calculation of Phébus-FPT3. It was pointed out that before when the paper published (2003), there was no B_4C control rod degradation model existed in the ICARE/CATHARE code. The paper presented at the first time the developed B_4C model in the ICARE/CATHARE code.

During last 10 years, Steinbrück and Steiner et al. at FZK have published valuable experiment results and mathematical modeling on the oxidation of B_4C at high temperatures.

(1) Steinbrück [24] investigated the oxidation kinetics of various types of B_4C (pellets and powder) in the temperature range between 800 and 1600 ºC. It was concluded that oxidation of B_4C was controlled by the formation of superficial liquid boron oxide and its loss due to the reaction with surplus steam to volatile acids and/ or direct evaporation at temperatures above 1500 ºC. The overall reaction kinetics was paralinear. Linear oxidation kinetics was established soon after the initiation of oxidation under the test conditions.

(2) Steiner [25] developed a simple parametric model for the simulation of B_4C oxidation tests at high temperatures at FZK. The model predicted that an equilibrium oxide film thickness was reached, whose value was only determined by the two rate parameters of the model. Applying the principles of convective mass transfer in coolant channels, one was able to establish the link from the parametric model to a more generalized consideration, which was allowed to identify the hydrogen surface concentration as a parameter, and this process was independent on the flow conditions.

(3) Based on the experimental data obtained in isothermal tests, Steinbrück et al. [26] developed a new model on B_4C oxidation. The model self-consistently simulated surface reaction kinetics and mass transport of various species in the multi-component gas phase as rate determining steps of the oxidation process. The model was implemented in the SVECHA/QUENCH code and verified against the transient test.

(4) On basis of extensive tests, Steinbrück [16] investigated the formation of B_4C-bearing melts and oxidation of the melt. Oxidation of the melts leaded to the production of CO, CO_2, and boric acids and to a significant additional release of hydrogen. The melts oxidized much faster than solid materials at the same temperatures because of fragmentation and the development of non-protective scales.

(5) Steinbrück [4] summarized the current knowledge on B_4C behavior during severe accidents mainly based on experiments performed at KIT. B_4C initiated local, but significant melt formation in the core at temperatures around 1250 ºC due to eutectic interactions with the surrounding steel structures. The B_4C-containing melt relocated and hence transported material

and energy to lower parts of the fuel bundle. The absorber melt was oxidized by steam very rapidly.

Simultaneously, IRSN has been performed a series of experiments to investigate the B_4C oxidation process. Accordingly, mathematical models were developed and applied in corresponding severe accidents codes.

(1) Seiler et al. [27] proposed a basic correlation, involving global variables, which had been developed for the simulation of boron carbide oxidation with the ICARE/CATHARE code. This modeling had been based on available experimental data, including VERDI separate effect tests performed by IRSN at low pressures and high temperatures. According to the agreement between the measured and the calculated bundle temperatures as well as hydrogen release and oxidized B_4C, the ICARE/CATHARE code simulates rather well QUENCH experiments involving B_4C control rod degradation, Zircaloy oxidation under starvation and cooling with steam.

(2) Dominguez et al. [28] investigated the oxidation kinetics of B_4C pellets in steam/argon mixtures in the temperature range 1200 – 1800 ºC for steam partial pressure between 0.2 – 0.8 bar and total flows (steam + argon) between 2.5 – 10 g/min resulting in gas velocities from 1.01 to 5.34 m/s. A kinetic model for B_4C oxidation depending on temperature, steam partial pressure and flow velocity is obtained. The activation energy of the oxidation process was determined to be 163±8 kJ/mol. The strong influence of temperature and steam partial pressure on the B_4C oxidation kinetics was confirmed. The obtained data suggested the coexistence of two kinetic regimes, one at 1200 ºC and the other at 1400 – 1800 ºC, with different dependence on steam partial pressure.

(3) Repetto et al. [29] described the progresses achieved in the frame of the Network of Excellence SARNET concerning the B_4C control rod degradation modeling in severe accident codes, such as ATHLET-CD, ICARE2, ASTEC, MELCOR and MAAP. It was revealed that large improvements of the kinetic correlation for B_4C oxidation were obtained from analytical experiments performed at FZK and IRSN, mostly in temperature range above 1127 ºC. Concerning the control rod degradation, SA codes such as ICARE2 and ATHLET-CD, using suitable modeling of B_4C oxidation, predicted rather well the total carbon release, for Phébus PFT3 in-pile experiment and QUENCH-07 and -09 out-of-pile experiments. Codes still have some difficulties to reproduce the final degradation of fuel bundles involving B_4C rods. Spreading of molten materials from the control rods onto fuel rods of the bundle is suspected, suggesting that the main effect of the B_4C control rod materials on the bundle behavior during degradation is connected with B_4C-SS eutectics formation and B_4C-SS-Zry liquid mixture relocation. These phenomena are not accounted for in current severe accident codes.

(4) Haste et al. [30] discussed recent integral and separate-effect tests performed at IRSN Cadarache and KIT relevant to oxidation and degradation of B_4C control rods under severe accident conditions. The integral Phébus FPT3 and QUENCH-07 and -09 experiments reinforced the existing database regarding the accelerated degradation of fuel rods due to spreading of

chemically aggressive eutectic melts for failed B_4C control rods onto neighboring fuel rods. The separate-effect tests gave quantitative data that were being used for development of detailed material interaction and oxidation models in severe accident codes such as ASTEC. These separate-effect tests were BECARRE program (by IRSN), and BOX, LAVA, QUENCH-SR (by KIT).

(5) Dominguez [31] investigated the oxidation kinetics of B_4C-SS liquid mixtures exposed to argon/steam atmospheres at temperatures up to 1527 ºC. A B-Cr-S-O liquid protective layer formed on the surface of the mixtures in contact with steam. This protective layer gradually transforms in to a Cr_2O_3-rich slag. Important quantities of liquid could be projected from the melt during oxidation. There projections were favored by high B_4C contents in the melt, high steam partial pressures and low temperatures. In addition, other compositions were studied in order to identify the basic oxidation mechanisms.

(6) de Luze [1] gave a code-based interpretation of the experimental BECARRE program carried out at IRSN between 2005 and 2010, using the severe accident code ASTEC/ICARE. Steam oxidation of solid B_4C pellets (at 1200 – 1800 ºC), as well as oxidation of molten B_4C bearing mixtures up to 9wt% of B_4C dissolution (at 1289 – 1527 ºC) were studied. A degradation test of 60 cm-long control rod segments was conducted, representative of a PWR geometry. The oxidation rates of the B_4C-bearing melts had been found always lower than the rates of the solid pellet oxidation in similar conditions, as modeled in ASTEC. It should be emphasized that this result is different from the result published by Steinbrück M. 2010. It was also shown that for temperature above 1600 ºC, the main effect of the B_4C was more toward a mitigation of the hydrogen production rather than increasing it by additional oxidation of boron compounds. No large increases of hydrogen release after the failure of the guide tube had been measured, due to downward relocation of the low viscosity B_4C-bearing melts. The ZrO_2 oxide layer formed on the outer surface of the guide tube had been found very protective.

(7) de Luze et al. [17] published the early phase fuel degradation in Phébus FP tests. According to the information of “early degradation phase” provided by de Luze et al., the degradation of the control rod and the oxidation runaway due to the fast oxidation of the Zircaloy claddings of the fuel rods, were two major events which took place. The first issue is the concerned phenomenon in this report, which includes the eutectic reaction (which is introduced previously) and the oxidation process. It was clarified that the kinetics of oxidation of bare solid B_4C pellets were well known, but the oxidation laws of B_4C materials coming out from a degraded control rod were more complex. General descriptions of solid B_4C pellets and B_4C-bearing melts oxidation were made in the paper. Comparison with BECARRE tests was also made in terms of carbonaceous gases and hydrogen.

2.3 Summary

Under the condition of severe accidents, the phenomena related to B_4C control rod consists of two aspects: eutectic interaction between B_4C-stainless steel and B_4C-Zircaloy, oxidation of intact B_4C pellet and B_4C-bearing melt. Literature review has been performed in this section. It can be summarized as follows. Integral experiments and separate effect tests have been performed worldwide, which are shown in Table 1 and Table 2, respectively.

(1) Kinetic functions of eutectic interaction between materials were investigated mainly in separate tests during 1990s. In 2000s, experiments at IRSN (Phébus FPT3) and KIT (LAVA furnace) confirmed previously obtained data and developed models for severe accident codes application.

(2) The investigation on oxidation kinetics started 1960s. During 1980s, some important results and correlations were developed for temperatures below 1300 ºC. The important paper by Belovsky (1995) revealed the start of research of B_4C oxidation under severe accident conditions. Integral experiments and separate effect tests have been performed mainly at IRSN and KIT.

(3) On the basis of experiment data, mathematical models have been developed and applied in different severe accident codes, for instance, ATHLET-CD, ICARE2, SCDAP/RELAP5, SVECHA/QUENCH, ASTEC, MELCOR and MAAP.

(4) Since 2012, investigation on the modeling of B_4C-bearing melt started and efforts for code application have been performed at IRSN and KIT, however, until now, there are no certain conclusions and mathematical models.

(5) The relocation process of B_4C-bearing mixture is still unknown, which would be a challenging point for severe accident code development, and it is assumed that the relocation both inside and outside of guide tube will affect the oxidation of B_4C-bearing melt.

Table 1 Integral experiments on B_4C control rods degradation [17]

Test	Rods	Failure temperature, ºC
ACRR-DF4	Blade	1250-1300 (relocation)
CORA-16	Blade	1200-1300
CORA-28	5 rods	1000-1200 (pressure loss)
	1 rod	>1520 (pressure loss)
	4 rods	1370 (temperature deviations)
CORA-W2	Centre	1220 (pressure loss)
QUENCH-07	Centre	1300 (He detection) 1310 (CO detection)
QUENCH-09	Centre	1280 (He detection) 1560 (CO detection)
Phébus FPT3	Centre	1450 (guide tube temperature) 1510 (CO detection)

Table 2 Recent separate effect tests on B_4C in terms of eutectic interaction and oxidation

Program	Facility	Affiliation
COLOSS (2000-2003)	BOX rig (KIT) TG rig (Krauss W., et al., 2003. KIT) LAVA furnace (KIT) QUENCH-SR rig (KIT) VERDI furnace (IRSN)	5th Euratom Framework Program (2000-2003)
BECARRE (2005-2010)	VERDI furnace PICCOLO furnace INTERMEZZO furnace	IRSN, the framework of the International Source Term Program (ISTP)

3 Modeling of B_4C-Related Eutectic Interaction and Oxidation for Severe Accident Codes

This section describes progresses concerning the B_4C control rod degradation and materials oxidation modeling in severe accident codes, such as ATHLET-CD, ICARE2, SCDAP/RELAP5, SVECHA/QUENCH, ASTEC, MELCOR and MAAP. The development of lumped parameter model in codes can combine improvements made in large- and small-scale experiments. Modeling of B_4C-involved reactions can reduce uncertainties in core degradation analysis, with the consideration of the release of extra energy, carbon gases, etc. The same to the previously summarized literature review, two processes are separately modeled in severe accident codes:

(1) Eutectic interaction of B_4C and other materials;

(2) Oxidation of intact B_4C and B_4C-bearing melt.

3.1 Eutectic interaction modeling

Since 1990s, separate effects tests were performed to investigate the eutectic interaction between B_4C-SS and B_4C-Zircaloy, and recently performed integral experiments (QUENCH and Phébus FPT3) proved those phenomena and corresponding correlations. The modeling of eutectic interaction in severe accident codes is summarized in this section. The correlation of perfectly contacted B_4C-SS pellet is valuable for mathematical model. Moreover, the mechanical degradation of control rod as a result of eutectic effect is also important, but this process as well as simultaneous mixture oxidation is still unknown and difficult to be modeled in current severe accident codes.

3.1.1 Background

Kinetics correlations for the eutectic interaction between B_4C and other materials should be included in the development of severe accident code. Different correlation functions based on experiments are introduced in this section. These correlations can be found in various severe accidents codes nowadays.

It was found at JAERI that the eutectic reaction between B_4C and other materials generally obeyed parabolic rate laws [9]. Kinetics for material interactions were summarized in Table 3. In some publications, this correlation was named as JAERI correlations [32].

Table 3 Kinetics for materials interaction at JAERI

Reaction system	**Temperature range (ºC)**	**Kinetics** $K\left(m^2/s\right)=K_0e^{-\frac{Q}{RT}}$	**Applicable temperature range (ºC)**
SS-304 / B_4C	800-1350	$K=1.49\times10^{-2}e^{-\frac{250000}{RT}}$ $K=1.40\times10^{10}e^{-\frac{549000}{RT}}$	800-1200 1125-1350
Zry-4 / B_4C	900-1680	$K=2.42\times10^{-8}e^{-\frac{173000}{RT}}$ $K=8.79\times10^{43}e^{-\frac{1965000}{RT}}$	900-1500 1225-1350
Zry-4 / (20wt% - B_4C + 80wt% - SS - 304)	1200-1650	$K=7.04\times10^{-9}e^{-\frac{41300}{RT}}$ $K=7.01\times10^{10}e^{-\frac{666000}{RT}}$	1200-1400 1500-1650

* $R=8.314\,J/mol/K$, Q: activation energy in J/mol .

Two years later than the publication of so-called JAERI correlations, Nagase et al. [10, 11] published updated correlations for B_4C/Zircaloy and B_4C/SS, respectively.

(1) B_4C and Stainless steel (SS-304)

The overall reaction between B_4C and stainless steel generally obeyed a parabolic rate law. An obvious discontinuity in the temperature dependence of the parabolic rate law constants was seen at the temperature level between 1200 ºC and 1225 ºC. This could be attributed to the formation of the liquid phase at the reaction interface.

B_4C pellet / SS reaction:

$$K\left(m^2/s\right)=1.49\times10^{-2}e^{-\frac{250000}{RT}},\ 800\ to\ 1200\ °C \tag{1}$$

$$K\left(m^2/s\right)=1.40\times10^{10}e^{-\frac{549000}{RT}},\ 1225\ to\ 1350\ °C \tag{2}$$

B_4C powder / SS reaction:

$$K\left(m^2/s\right)=3.04\times10^{-1}e^{-\frac{283000}{RT}},\ 800\ to\ 1200\ °C \tag{3}$$

$$K\left(m^2/s\right)=3.15\times10^{7}e^{-\frac{453000}{RT}},\ 1225\ to\ 1350\ °C \tag{4}$$

(2) B_4C and Zircaloy-4

The overall reaction generally obeyed a parabolic rate law which is the same to that of B_4C

and SS. A sudden increase of the reaction rate was found at a temperature between 1550 and 1600 ºC. The discontinuity in the temperature dependence of the parabolic rate law constants at a temperature between 1550 and 1600 ºC could be attributed to the localized liquid phase formation at the reaction front.

For the reaction layer growth:

$$K\left(m^2/s\right)=4.10\times10^{-8}e^{-\frac{179000}{RT}},\ 800\ to\ 1550\ °C \tag{5}$$

$$K\left(m^2/s\right)=6.74\times10^{43}e^{-\frac{1960000}{RT}},\ 1600\ to\ 1680\ °C \tag{6}$$

For the decrease in Zircaloy thickness:

$$K\left(m^2/s\right)=3.74\times10^{44}e^{-\frac{1988000}{RT}},\ 1600\ to\ 1680\ °C \tag{7}$$

At FZK in Germany, Veshchunov and Hofmann [12, 13] performed experiments on the same subject and correlations were obtained independently. It should be emphasized that temperatures in Veshchunov's experiments were lower than that in Nagase's.

(1) B_4C and Stainless steel 1.4919 (AISI 316)

Results of detailed chemical-analytical examinations of B_4C/SS reaction couples obtained at temperatures of 1000, 1100, and 1200 ºC.

$$K\left(m^2/s\right)=8.76\times10^{2}e^{-\frac{378000}{RT}}\ 1000\ to\ 1200\ °C \tag{8}$$

(2) B_4C and Zircaloy-4

$$K\left(m^2/s\right)=2.38\times10^{-8}e^{-\frac{170840}{RT}}\ 800\ to\ 1500\ °C \tag{9}$$

Belovsky et al. [2] summarized the results of experiments with short PWR control rod segments, containing B_4C, in accident conditions. The reaction behavior between the B_4C (pellets or powder), AISI-304 stainless steel and Zircaloy-4 tubes was studied and correlations were proposed. Experimental temperature range was 800 to 1500 ºC. These correlations were referred as Belovsky correlation in Austregesilo et al. [32] The possible relocation of liquid phases at higher temperature would be invoked rather by cracking of the Zircaloy-4 guide tube due to mechanical loads than by the chemical liquefaction of the guide tube, so the B_4C/Zircaloy-4 model was not developed in Belovsky's papers. The modified B_4C/SS model was compared with original ICARE2 B_4C/SS model.

(1) B_4C and Stainless steel (AISI-304)

B_4C pellet / SS reaction:

$$K\left(m^2/s\right)=5.0\times10^{20}e^{-\frac{850000}{RT}}\ 1210\ to\ 1340\ °C \tag{10}$$

B_4C powder / SS reaction:

$$K\left(m^2/s\right)=4.6\times10^{11}e^{-\frac{544000}{RT}}\ 1210\ to\ 1340\ °C \tag{11}$$

3.1.2 MELCOR

MELCOR is a fully integrated, engineering-level computer code that models the progression of severe accidents in light water reactors. MELCOR is being developed at Sandia National Laboratories for U.S. Nuclear Regulatory Commission as a second-generation plant risk assessment tool and the successor to the Source Term Code Package [33].

Material properties of B_4C as a constituent of debris, including melting temperature (default = 2454.6 ºC), molecular weight (default = 55.260) and heat of fusion (1.89336E+06), are defined in MP (Material Properties) package. In MELCOR 1.8.5, the eutectic reaction temperature is used to define the temperature at which the rate of eutectic reaction between two contacting solids is sufficiently high to cause significant liquefaction on a time scale of interest. The threshold for eutectic reaction between B_4C powder and steel cladding is taken at 1247 ºC. However, there is no specific kinetics correlation of B_4C/SS eutectic interaction in MELCOR 1.8.5. There are three eutectic reactions considered in MELCOR 1.8.5: Zircaloy/Inconel; Zr/SS and B_4C/SS, which lead to the early failure of fuel and control rods. B_4C/Zircaloy eutectic interaction temperature is very high (1627 ºC) in MELCOR 1.8.5, which is used to decide the mixture solidus temperature and is not allowed to be changed as a sensitivity coefficient.

In MELCOR 1.8.6, the B_4C oxidation is allowed to commence when temperature exceeds 1227 ºC, and the material is allowed to fully liquefy and relocate when the temperatures exceeds 1427 ºC. This treatment is different from MELCOR 1.8.5, but it does not change the qualitative modeling of B_4C/SS interaction only by setting up threshold temperatures.

3.1.3 ICARE2 (ICARE/CATHARE)

The ICARE2 code is the stand-alone core degradation module of the ICARE/CATHARE code system developed by IRSN [34].

(1) B_4C/SS eutectic interaction

The modified Belovsky correlation is used in ICARE2. The parabolic correlation for B_4C pellets were added based on experiments with crucibles by Hoffman and Uetsuka. The B_4C/SS interaction is assumed as starting at 800 ºC and the transition temperature to the accelerated kinetics is set to 1210 ºC, above which the reaction rate will increase. Since ~6 wt% of carbon was detected in the reaction zone in the experiments by Hoffman and Uetsuka, the B_4C fraction in the B_4C/SS mixture simulating the reaction zone was increased from 5.5 wt% to 9 wt%.

(2) B_4C/SS/Zircaloy-4 eutectic interaction

In ICARE2, there is a model which calculates the liquefaction of Zircaloy by solid stainless steel. It is however not used in the calculation, mainly because the contact between the steel cladding and the guide tube is never met, a gap between guide tube and control rod cladding in PWR, not allowing the interaction to begin. Because of the lack of modeling of B_4C/SS/Zircaloy-4 eutectic interaction, it is assumed that the PWR control rod failure arises from an instantaneous Zircaloy dissolution by the molten B_4C/SS mixture. The melting of the SS (1450 ºC) is selected as the key-event that triggers the rupture of the control rod.

Two criteria are selected for the failure of the control rod. When either criterion is reached, the oxidation of B_4C will start.

- The SS cladding is totally dissolved by the B_4C (B_4C/SS interaction);
- The guide tube temperature is higher than 1450 ºC.

3.1.4 ATHLET-CD

The system code ATHLET-CD is being developed for best-estimate simulation of accidents with core degradation and for evaluation of accident management procedures. It applies the detailed models of the thermal-hydraulic code ATHLET in an efficient coupling with dedicated models for core degradation and fission products behavior [32].

In ATHLET-CD, three kinetics interactions are included [32], which are JAERI correlation, Belovsky correlation, and Nagase correlation. It is concluded from sensitivity analysis using ATHLET-CD that the modeling of B_4C/SS interaction and B_4C oxidation does not affect significantly the calculated global thermal behavior of the test bundle nor the total hydrogen generation. The main uncertainty parameter related to B_4C oxidation is the multiplication factor of surface area due to porosity.

3.1.5 MAAP

The Modular Accident Analysis Program (MAAP) is an Electric Power Research Institute (EPRI) owned and licensed software, which is a fast-running computer code. It can be used to simulate the response of light water reactors and heavy water moderated reactors for both current and advanced designs. MAAP4 is also used at Électricité de France (EDF) for severe accident modeling. One major revision in EDF version of MAAP is associated with the B_4C-AIC hybrid control rod degradation of French PWR design.

According to Repetto et al. [29], interaction of B_4C with surrounding materials is modeled in MAAP4: stainless steel cladding first, zircaloy guide tube later on. This interaction involves only a fraction of the actual amount of B_4C, since the eutectic B_4C-SS has a limited content in B_4C (assumed to be 9% in mass). However, the detailed model of B_4C/SS interaction was not available for authors.

3.2 Oxidation modeling for solid pure B_4C

Entering into the 2000s, the experimental database has been greatly improved in Europe based on COLOSS and SARNET projects. The improvements are reflected in the kinetic correlations of B_4C oxidation. New model can predict the total carbon releases rather well, which are confirmed in large scale experiments (Phébus FPT-3, QUENCH-07, and -09). Temperatures of interest for severe accident transient regarding B_4C oxidation are above 1300-1500 ºC when the failure of the stainless steel control rod tube has occurred [29].

3.2.1 Background

The extrapolation based on experimental data at low temperature ranges ≤ 1300 ºC [19-21] was found of large uncertainty, which was solved by additional experiment launched at IRSN and KIT. Experimental data at high temperature were obtained in several experiments.

The Liljenzin correlation assumed that the dependence of oxidation rate on temperature can be expressed by the Arrhenius law.

$$k = k_0 e^{-\frac{E_a}{RT}} \tag{12}$$

The Liljenzin correlation was later extended to take into account the influence of steam partial pressure and total pressure.

$$k = k_0 e^{-\frac{E_a}{RT}} P_{H_2O}^{\alpha} P_{Tot}^{\beta} \tag{13}$$

In Equations (12) and (13), the oxidation rates (k) dependency on temperature (T) are expressed by Arrhenius laws. k_0 and E_a are respectively the initial rate coefficient and equivalent activation energy. The oxidation rate dependency on steam partial pressure (P_{H_2O}) and total pressure (P_{Tot}) are taken into account with α and β coefficients. Equation (12) is the special form of (13) without taking into account the dependency on steam partial and total pressure ($\alpha = \beta = 0$). Table 4 provides parameters obtained from experiments. Each row represents the correlation obtained based on respective experimental data. The correlation of last row (IRSN 2006) in Table 4 was recommended to be used by Repetto G. Figure 1 also shows that the IRSN correlation accords with all historical experimental data rather well.

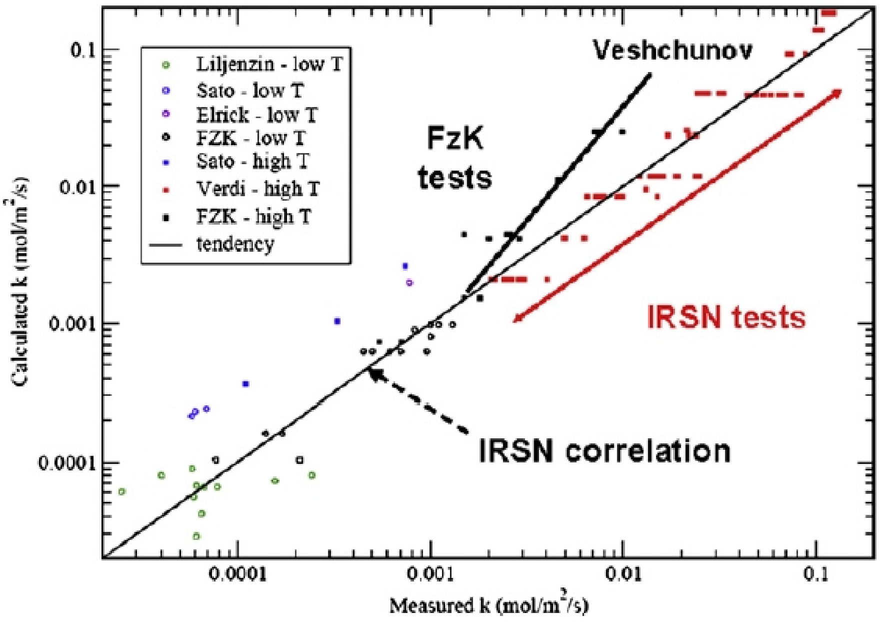

Figure 1 Comparison of oxidation kinetics rates between mathematical models and experimental data [29]

Table 4 Coefficients for B_4C oxidation kinetics [29]

	T (ºC)	**k_0 (mol $B_4C/m^2/s$)**	**E_α (10^5 J/mol)**	**α**	**β**
Liljenzin		3.29×10^{3}	1.81	0	0
Litz		5.29×10^{-9}	0.46	1	0
Sato		1.03×10^{2}	1.54	0	0
IRSN (2002)		34.17	1.6334	1.18	-0.78
IRSN (2004)		263.32	1.8587	0	-0.75
BOX data (FZK 6979)		6.81×10^{3}	1.887	0	0
VERDI data (GRS)		1.143×10^{3}	1.503	0	0
VERDI BOX data (GRS)	<1527	1.143×10^{3}	1.503	0	0
	>1527	1.471×10^{6}	2.586	0	0
FZK BOX data*		1.471×10^{6}	2.586	0	0
FZK BOX/TG data*		1.250×10^{6}	2.650	0	0
Veshchunov M.S. et al., 2005	<1100	2.5×10^{-7}	0.216	1	0
	>1100	6.0×10^{5}	3.829	1	0
IRSN (2006)	<1127	4.33×10^{-6}	0.25	1	-0.25
	>1127	3.64	1.775	1	-0.25

(1) Remark: these values are not usable for high pressure transients.

(2) * for B_2O_3 reduction.

The oxidation of B_4C by steam can be described by equations as follows. Under the condition of severe accidents, it will result in the formation of liquid boron oxide (B_2O_3), gaseous carbon species and hydrogen.

$$B_4C+7H_2O(g)\leftrightarrow 2B_2O_3(l)+CO(g)+7H_2(g) \tag{14}$$

$$B_4C+8H_2O(g)\leftrightarrow 2B_2O_3(l)+CO_2(g)+8H_2(g) \tag{15}$$

$$B_4C+6H_2O(g)\leftrightarrow 2B_2O_3(l)+CH_4(g)+4H_2(g) \tag{16}$$

$$B_4C+6H_2O(g)\leftrightarrow 2B_2O_3(l)+C+6H_2(g) \tag{17}$$

The resulting boric oxide can react with steam to form boric acid or be directly vaporized at high temperature and certain atmospheric pressure. A simple and preliminary modeling of linear kinetics assumption was found in related literatures and applied to early ICARE2 code. The model was used to perform Phébus FPT-3 pre-calculations in 2002. This simple model of B_4C oxidation is described as: the oxidation of one mole of B_4C consumes 10 moles of H_2O and releases 8 moles of H_2 [35]. Here, the model takes into account reactions for both B_4C oxidation and B_2O_3 consumption.

$$B_2O_3\left(l\right)+H_2O\left(g\right)\leftrightarrow 2HBO_2\left(g\right)\ \left(\text{metaboric acid}\right) \tag{18}$$

$$B_2O_3\left(l\right)+3H_2O\left(g\right)\leftrightarrow 2H_3BO_3\left(g\right)\ \left(\text{orthoboric acid}\right) \tag{19}$$

$$B_2O_3\left(l\right)+H_2O\left(g\right)\leftrightarrow 2/3\left(HBO_2\right)_3\left(g\right)\ \left(\text{trimer of metaboric acid}\right) \tag{20}$$

$$B_2O_3\left(l\right)\leftrightarrow B_2O_3\left(g\right) \tag{21}$$

In addition, three secondary reactions can probably take place in the gas phase.

$$CH_4\left(g\right)+H_2O\left(g\right)\leftrightarrow CO\left(g\right)+3H_2(\mathrm{g}) \tag{22}$$

$$CH_4\left(g\right)+2H_2O\left(g\right)\leftrightarrow CO_2\left(g\right)+4H_2(\mathrm{g}) \tag{23}$$

$$CO\left(g\right)+H_2O\left(g\right)\leftrightarrow CO_2\left(g\right)+H_2(\mathrm{g}) \tag{24}$$

3.2.2 MELCOR

Oxidation models applied in MELCOR 1.8.5 and 1.8.6 are compared in this section. The reaction of B_4C with steam is modeled in both MECLOR 1.8.5 and 1.8.6. It is depicted in the Users' Guide that the default B_4C oxidation model produces satisfactory results in highly oxidizing atmospheres, and that if significant hydrogen concentrations (reducing environments) are expected, the advanced B_4C reaction model should be invoked [33]. The simple default model was developed by Oak Ridge National Laboratory (ORNL) for the MARCON 2.1B code, and the advanced model was also developed by ORNL for BWRSAR code, which is the successor to MARCON code. It should be mentioned that oxidation models in MELCOR 1.8.5 and 1.8.6 are not largely different. The oxidation model in MELCOR 1.8.6 extends to enable PWR control rods to be represented [36].

Three initial parameters are important in the default B_4C oxidation model:

(1) Maximum B_4C fraction that may be consumed by the reaction (default = 0.02): Any B_4C material dissolved in the eutectic mixture is considered to be unavailable for reaction.

(2) Intact steel fraction: The B_4C reaction will begin when the ratio of the intact steel mass to its initial value falls below this fraction (default = 0.9).

(3) Reaction threshold temperature: When the B_4C temperature exceeds this value, the reaction can start (default = 1227 ºC).

According to users' guides of MELCOR 1.8.5, the B_4C oxidation rate can be represented by

$$\frac{d\left(M/M_0\right)}{dt}=1.662\times10^5 e^{-\frac{1.88299\times10^4}{RT}}=1.662\times10^5 e^{-\frac{2.26472\times10^4}{T}},\ T>1227\ °C \tag{25}$$

Here, M and T are respectively current B_4C mass and temperature, and M_0 is the initial B_4C mass. It should be emphasized that in the simple model, partial steam pressure and total pressure are not involved. According to Equation (25), the mass fractional change per second for B_4C can be obtained.

The next problem is to decide how much CO, CO_2, and CH_4 are released during each time step. In MELCOR code, oxidation reactions of B_4C include Equations (14) ~ (16). Chemical equilibrium of all reaction products is assumed, and the model uses the steam and hydrogen partial pressures and B_4C temperature to determine the relative extent of each reaction, which can be written as follows. The masses of C-compound gases and released energies can be calculated accordingly. The equilibrium CO/CO_2 and CO/CH_4 moles ratios are expressed as y_{CO/CO_2} and y_{CO/CH_4}, respectively. Partial hydrogen and steam pressure are expressed as P_{H_2} and P_{H_2O}, respectively.

$$y_{CO/CO_2} = \frac{P_{H_2}}{P_{H_2O}} e^{-\frac{3605.0}{T}+3.427} \tag{26}$$

$$y_{CO/CH_4} = \frac{P_{H_2O}}{\left(P_{H_2}\right)^3} e^{-\frac{27350.0}{T}+30.50} \tag{27}$$

The advanced B_4C reaction model in MELCOR 1.8.5 determines the equilibrium composition in each control volume that is achieved when the Gibbs free energy of the system is minimized. The difference between the initial composition in the control volume and the equilibrium composition determines the rate of consumption of the reactants. The governing function can be written as

$$\frac{G}{RT} = \sum_i n_i \left[\left(\frac{g^o}{RT} \right)_i + \ln\left(a_i\right) \right] \tag{28}$$

Here, G is the total free energy of the system; R is the gas constant; T is the thermodynamic temperature; n_i is the number of moles of the i$^{\mathrm{th}}$ species; g^o is the standard chemical potential; a_i is the corresponding activity.

The advanced B_4C reaction model assumes that chemical equilibrium is achieved between the reactants during each time step. The mass of B_4C available for reaction during each time step is determined by Equation (25), which is shared with the simple default B_4C reaction model.

Therefore, the simple model considers formation of B_2O_3 and partitioning formation between CO, CO_2 and CH_4 formation. The advance model considers thermodynamic equilibrium between these products and HBO_2, $H_3B_3O_6$, BOH, BH_3, B_2H_6, O, B and C. However, it is commented by Repetto et al. [29] that “the advanced model appears to offer no advantage despite the added complexity”. The comment seems reasonable because of two reasons.

(1) Even though the advanced model takes into account of more materials and the effect caused by hydrogen-rich environment, the B_4C oxidation correlation is not improved.

(2) One important reason why the advanced model is applied is that the simple default model tends to underestimate the production rate of methane [33, 36], which has been proved as negligible in QUENCH -07, 09 and Phébus FPT3 experiments, etc.

The oxidation correlation is not changed in MELCOR 1.8.6, but the so-called new B_4C control rod oxidation model by Gauntt et al. [36] takes into account of the oxidation of eutectic mixture, which can more mechanistically represent the B_4C oxidation than the simple fractional oxidation treatment. Comparison between original model and new model was made based on numerical calculations. According to the Testdemo comparison between the original model and the new one, the new one generated relatively more B_2O_3 and releasing timing of B_2O_3 was also different. It is concluded by Gauntt et al. [36] that the new model was believed to arrive at this result from a more mechanistic standpoint.

3.2.3 ICARE2 (ICARE/CATHARE)

The basic correlation, involving global variables, has been developed for the simulation of B_4C oxidation with the ICARE/CATHARE code. It is emphasized again that the development of the correlation involved the VERDI separate effects experiments by IRSN at low pressures and high temperatures. According to the publication [27], ICARE/CATHARE code simulated rather well QUENCH experiments involving B_4C control rod degradation, so that the model validation work seemed to be well-done.

In ICARE/CATHARE, after the failure of the B_4C control rod, the oxidation of B_4C can start. The kinetics correlation used the same to the background introduction in Section 3.2.1. The Arrehnius law with IRSN (2006) defined parameters is used. According to Seiler N., the model introduction and corresponding validation work are introduced as follows.

$$\begin{cases} T < 1123°C,\ k = 4.33\times10^{-6} e^{-\frac{2.5\times10^{4}}{RT}} P_{H_2O}^{1} P_{Tot}^{-0.25} \\ T > 1123°C,\ k = 3.64 e^{-\frac{1.775\times10^{5}}{RT}} P_{H_2O}^{1} P_{Tot}^{-0.25} \end{cases} \tag{29}$$

(1) Steam partial pressure: according to Veshchunov et al. [37], the dependence of oxidation rate on steam partial pressure is assumed to be linear ($\alpha = 1$);

(2) Total system pressure: since most experiments have been done at atmospheric pressure, the dependence of oxidation rate on system pressure is not highlighted in the tests. In ICARE/CATHARE, the existence of such dependence is still assumed;

(3) Temperature: the dependence of oxidation rate on temperature is also expressed as an Arrhenius law. Because of the existence of boron oxide reduction process (chemical reaction with steam and direct evaporation), there will be a significant change of oxidation rate at temperature range (1023 – 1223 ºC). The reason can be explained: due to a strong temperature dependence of boron oxide evaporation, very high rates are measured for high temperatures, whereas indirect transport

via boric acids would dominate at lower temperatures.

When the system hydraulics is taken into account at high temperature range, the correlation can be given by as follows, which is restricted to the VERDI's experimental conditions [27].

$$\begin{cases} T < 1123°C,\ k = 4.33\times10^{-6} e^{-\frac{2.5\times10^{4}}{RT}} P_{H_2O}^{1} P_{Tot}^{-0.25} \\ T > 1123°C,\ k = 2.35 e^{-\frac{1.775\times10^{5}}{RT}} P_{H_2O}^{1} P_{Tot}^{-0.25} \mathrm{V}_f^{0.29} \end{cases} \tag{30}$$

Here, $V_f\left(m/s\right)$ is the flow velocity of gases.

The validation work of ICARE/CATHARE code was done towards QUENCH series tests. Calculation results simulated experiments rather well, especially up to the cool-down phase under steam starvation and cooling conditions.

3.2.4 ATHLET-CD

Totally 7 correlations have been implemented in ATHLET-CD code for B_4C oxidation rate, and 2 correlations have been implemented for the B_2O_3 reduction rate. All the correlations are shown in Figure 2. Austregesilo et al. [32] conducted sensitivity analysis for H_2 production involving selection of B_4C oxidation model but B_2O_3 reduction model was not involved. Base cases were set up with B_4C oxidation correlation from VERDI and BOX experiments (R1(7)), and B_2O_3 reduction model from BOX and TG data (R2(2)).

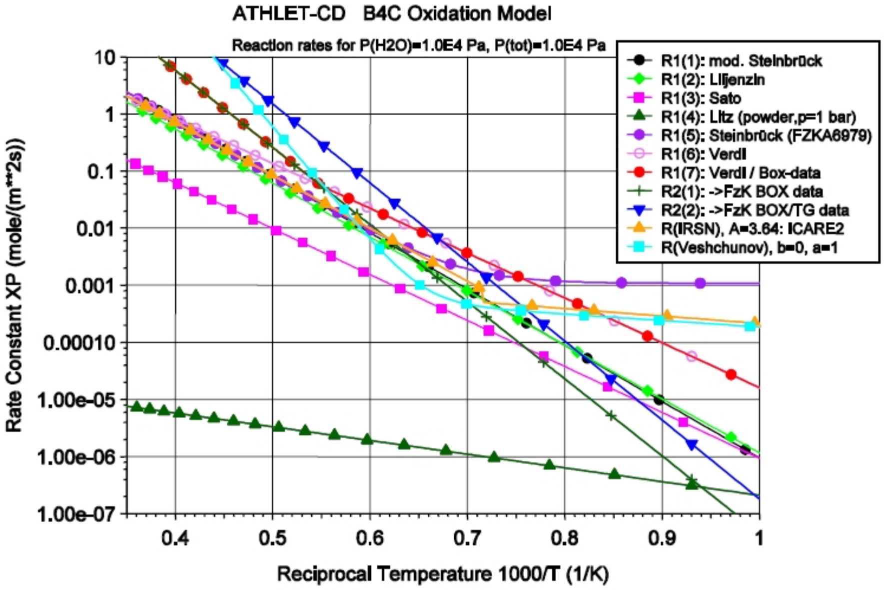

Figure 2 Oxidation kinetics law used in ATHLET-CD code

3.2.5 MAAP

The combination of models (eutectic interaction of B_4C and other materials, pure B_4C oxidation model, relocation of B_4C-SS mixture, oxidation of melt) is in the future development of MAAP code. EDF revised version of MAAP4.04 included three empirical oxidation laws which are introduced previously [29].

1. MELCOR correlation: The correlation is provided in Section 3.2.2 with Equation (25).
2. FZK correlation: This correlation is based on data from BOX test and is shown in row 6, Table 4.
3. IRSN correlation: This correlation is from ICARE2 in Section 3.3.3 with Equation (29), which was validated against data from BOX and VERDI tests.

The product equilibrium is also assumed in order to evaluate probability fractions of Equation (14) ~ (16). This process is same to that in MELCOR 1.8.5.

3.2.6 SVECHA/QUENCH

Veshchunov et al. [37] developed new models and applied it in SVECHA/QUENCH code. This model was verified based on BOX rig test results. The main inconsistency of other B_4C oxidation models was eliminated. Results show that a more precise solution for hydrogen release and additionally, a chemical composition of the outlet gas mixture, can be calculated by this model. The SVECHA/QUENCH code was also applied to the simulation of QUENCH-07. Numerical results also show good agreement with that of experiments.

$$\frac{dN_{B_4C}}{dt} = \alpha\left(T\right) P_{H_2O}^{a} P_{tot}^{b} \tag{31}$$

$$\alpha\left(T\right) = K_1 e^{-\frac{E_1}{RT}} + K_2 e^{-\frac{E_2}{RT}} = 2.5\times10^{-7} e^{-\frac{21600}{RT}} + 6.0\times10^{5} e^{-\frac{382900}{RT}} \tag{32}$$

3.3 Oxidation modeling for B_4C-bearing mixture

Almost all severe accident codes do not involve the detailed modeling of the oxidation of B_4C-bearing mixtures. For instance, B_4C in eutectic mixture is not allowed to be oxidized in MELCOR 1.8.5 and 1.8.6; kinetics correlations of solid B_4C oxidation are used to envelop B_4C-bearing mixtures in ICARE2. Therefore, in this section, currently conducted experiments are reviewed.

Two interesting phenomena have been found in two independent experiments [16, 1]. Steinbrück concluded that the experiments performed with prototype control rod segments indicated very high oxidation rates of the absorber-metal melts released after failure of the oxidized Zircaloy guide tube. On the other hand, de Luze found that the oxidation rates of the B_4C bearing melts were always lower than the rates of the solid pellet oxidation under similar conditions. No large increases of the hydrogen release after the failure of the guide tube were measured, due to downward relocation of the low viscosity B_4C bearing melts inside the 60 cm-height control rod segments. The ZrO_2 oxide layer formed on the outer surface of guide tube was very protective, leading to failure only above 1650 ºC. Details of mixture oxidation are shown as follows.

(1) Experiments at KIT in Germany (Steinbrück)

Steinbrück et al. [15] depicted the experimental details. Three experimental setups were used for the investigation of degradation and oxidation of B_4C control rod segments at high temperatures at KIT in Germany: the BOX rig, the single-rod QUENCH-SR rig, and the LAVA furnace. The BOX rig was used to perform tests with small, one-pellet-size specimens as well as the oxidation tests with absorber melts. The QUENCH-SR rig was used for tests with longer, about 10 cm control rod segments. The LAVA furnace was used to analyze SS/ B_4C/Zircaloy-4 melts and also was used for B_4C/SS dissolution tests.

In the BOX rig, liquid interaction layers are generated between Zircaloy and solid steel and between B_4C and steel. After the failure of the external oxide shell (ZrO_2), significant oxidation rate of B_4C pellet was found. In the QUENCH-SR rig, it was also found that the ZrO_2 scale protected the B_4C pellets and the absorber melt inside from steam as long as it was intact. Only after the failure of the oxide shell, B_4C was oxidized locally near the position of the oxide failure. The experiments performed on prototype control rod segments indicated very high oxidation rates of the absorber-metal melts released after failure of the oxidized Zircaloy guide tubes. Therefore, separate-effects tests on the oxidation of such melts were conducted in the LAVA furnace. The composition of the melt, especially its melting point, has a strong influence on oxidation kinetics. Key results obtained in three facilities are shown in Table 5. For French design control rods, the temperature dependent behaviors are described in Table 6.

Table 5 Key results obtained in experiments at KIT

Experimental facility		**Minor interaction**	**Significant melt production**	**ZrO_2 layer failure**
BOX rig	Metal plugs	1200 ºC	1400 ºC	1700 ºC
	Ceramic caps	1200 ºC	1300 ºC	1500 ºC
QUENCH-SR rig		1040 ºC	N/A	1470 - 1580 ºC
LAVA furnace		Decided by the composition of the mixture (800 - 1550 ºC)		

Table 6 Behavior of a French PWR design in dependence as a function of temperature

Temperature	**Behavior**
1000 ºC	No significant interactions of stainless steel, boron carbide and Zircaloy
1200 ºC	Local interactions of stainless steel, boron carbide, and Zircaloy (see Section 3.1 for kinetics correlations)
≥ 1250 ºC	Rapid, complete liquefaction of metals (steel, Zircaloy) in the gap between B_4C pellet and external ZrO_2 scale
≥ 1450 ºC	Failure of the oxide scale and rapid oxidation of absorber melt and remaining B_4C pellets

(2) Experiments at IRSN in France (de Luze)

Based on BECARRE program, the oxidation of B_4C-bearing melt was investigated by de Luze, and BECARRE program was composed of three main phases.

Phase I: solid B_4C pellets oxidation (at 1200 - 1800 ºC);

Phase II: oxidation of B_4C bearing mixtures (9 wt% of solid B_4C at 1289 - 1527 ºC);

Phase III: degradation of 60 cm long B_4C control rod (60 cm long control rod of French PWR geometry, ~ 2000 ºC).

It was pointed out that the molten mixture containing B_4C could lead to non-negligible additional gas releases, but the correlations for the oxidation of the B_4C bearing mixture were still insufficient.

Based on BECARRE Phase II results, the chemical reaction model of B_4C-bearing mixture is irrelevant. However, experimental releases and those given by the correlation for the oxidation of the solid B_4C pellets were in the same range of order. Therefore, no specific modeling for the oxidation rates of boron under molten B_4C/SS mixture has been done in ICARE, still using the solid correlation for an envelope calculation.

Based on BECARRE Phase III, the large increase of the oxidation rates was due more to a scale effect of the tests rather than a large increase of the oxidation rates of the B_4C bearing melts. The explanation was provided in the publication. The impact of the rod-type B_4C against oxidation and the following hydrogen release was found to be lower than expected, with evidences of a mitigation of the releases, due to the downward relocation of the melts and to dissolution effects with less Zircaloy being oxidized.

4 Models applied to THALES-2

In Sections 2 and 3, the current progress of B_4C-related experiments and modeling has been summarized. In this section, important experimental conditions are selected and compared, and appropriate models are recommended to be applied to THALES-2. This section aims at evaluating which correlation is the most meaningful one to be applied to the numerical modeling process.

4.1 Comparison of experimental conditions

According to materials introduced before, two types of experiments have been conducted to investigate the phenomena of B_4C rod degradation and oxidation. Mechanistic and kinetic information gained from separate effects tests are important in the development of corresponding physical models and codes. The correlations can be validated by the comparison between calculated results (pre- and post-experiment) and experimental results.

Conditions of important experiments are summarized in Table 7 and Table 8 for eutectic interaction and oxidation, respectively. All of the information shown in these tables can be used to compare with accident conditions including Fukushima Daiichi NPS accident.

Table 7 Experimental conditions for eutectic interaction

Author	**Experiments or document**	**Lab.**	**Materials**	**Temperature range**	**Reaction kinetics**	**Scale**
Hofmann et al.	KfK4598 (1989) [5]	KfK	B_4C (powder)/SS (AISI 316); B_4C (powder)/Zircaloy-4 (Zry-4).	800 – 1200 ºC 800 – 1600 ºC	Parabolic rate laws	SET
Gauntt et al.	DF-4 (1989) [7]	SNL	Bundle test with fuel rods, Zircaloy-4 fuel canister, stainless steel (SS316), and B_4C(powder)	~ around 1800 ºC	N/A	Integral
Sepold et al.	CORA-16, 17 and 18 (1988-1990) [8]	KfK	Bundle test with fuel rod simulators and absorber rods with steel and B_4C(powder)	1200 – 2000 ºC (CORA-18, ~ 1900 ºC)	N/A	Integral
Uetsuka et al.	(1995) [9]	JAERI	SS-304/B_4C (ceramics) Zry-4/B_4C (ceramics) Zry-4/(20wt%-B_4C+80wt%-SS304) (ceramics)	800 – 1350 ºC 900 – 1350 ºC 1200 – 1700 ºC	Parabolic rate laws	SET
Nagase et al.	(1997) [10, 11]	JAERI	SS-304/B_4C (powder and pellet) Zry-4/ B_4C (powder and pellet)	800 – 1350 ºC 900 – 1680 ºC	Parabolic rate laws	SET
Belovsky et al.	(1997) [2]	Czech Republic	SS (AISI 304)/B_4C (powder and pellet) SS (AISI 304)/B_4C (pellet)/Zry-4	800 – 1500 ºC	Parabolic rate laws	SET
Steinbrück et al.	LAVA furnace, COLOSS program (2004, 2010) [15, 16]	KIT (FzK)	SS (AISI 304)/B_4C specimens with large (5 wt%), medium (1 wt%), and small (0.3 wt%) B_4C pellet	~ around 1250 ºC	N/A (qualitative description)	SET
de Luze and Barrachin	Phébus FPT-3 (2013) [17]	IRSN	Bundle test with B_4C control rod	~ 2000 ºC	N/A	Integral

Table 8 Experimental conditions for oxidation (1/2)

Authors / Experiments	**Materials**	**Temperature range**	**Gas inflow rate**	**Pressure**	**Reaction kinetics**	**Scale**
Elrick,Sato,Liljenzin [19-21]	B_4C pellets and powder	854 – 1300 ºC	N/A	$P(H_2O) = 0.01–0.1$ bar; P(total) = 0.01 – 1 bar.	Parabolic rate laws	SET
Belovsky et al. [22]	B_4C powder, high-dense hot-pressed B_4C	Data from previous experiments	N/A	N/A	Parabolic, then linear (B_2O_3 formation & consumption)	SET
COLOSS [3, 23]*	B_4C (BWR, VVER, and PWR)	1200 – 1800 ºC	Total (steam + Ar): 2 – 10 g/min	$P(H_2O) = 0.2 – 0.9$ bar.	Parabolic B_2O_3 formation & linear B_2O_3 evaporation, etc.	SET & Integral
VERDI [3, 23, 28]	B_4C pellet	1200 – 1800 ºC	Total (steam + Ar): 2.5 - 10 g/min	$P(H_2O) = 0.2 - 0.8$ bar; P(total) = 1 bar.	Parabolic, then linear (B_2O_3 formation & consumption)	SET
BOX rig [24, 26, 38]	B_4C pellet and powder SS/B_4C/Zry-4 (10 types of absorber melts)	800 – 1600 ºC	Steam: ~ 90 g/h (30 g/h at normal conditions); Ar: ~ 90 l/h (50 l/h at normal conditions).	$P(H_2O) = \sim 0.79$ bar; P(total) = 1 bar (normal condition).	Paralinear overall reaction kinetics	SET
TG-rig [39]	B_4C pellet and powder	600 – 1300 ºC	Ar/O_2: 10 lh Ar/H_2O: 10, 20 l/h	$P(H_2O) = 0.012$ bar, 0.1 bar, etc.	Paralinear overall reaction kinetics	SET
QUENCH-SR [15]	10 cm B_4C control rod	1040 – 1600 ºC	Steam: 100 g/h; Ar: 100 l/h	N/A	Paralinear overall reaction kinetics	SET

Table 8 Experimental conditions for oxidation (2/2)

BECARRE [1]	B-I: Solid B_4C pellets; B-II: B_4C-bearing mixture; B-III: 60 cm B_4C control rod	B-I: 1200-1800 ºC B-II: 1289-1527 ºC B-III: ~2000 ºC	B-I: Total (H_2O+Ar): 2.5 – 10 g/min; B-II: Steam: ~ 60.5 g/h B-III: 360 g/h (no steam starvation)	B-I: P(H_2O) = 0.2 – 0.8 bar; P(total) = 2 bar. B-II: P(H_2O) = 0.43 bar B-III: P(H_2O) = 0.8 bar	Paralinear overall reaction kinetics (pellet)	SET
CORA [8, 40]	Bundle test with B_4C control rods (CORA-16, 17, 18)	1200 ºC – 2000 ºC (a few cases up to 2400 ºC)	Ar: 8 g/s or 16 g/s (18); Steam: 2 g/s or 4 g/s (18).	P(total) = 2.2 bar.	N/A	Integral
QUENCH-07 [41, 42]	B_4C control rod	~ 2047 ºC	Ar: 3 g/s; Steam: 3 g/s.	P(total) = 2 bar.	N/A	Integral
QUENCH-09 [43]	B_4C control rod	~ 2047 ºC	Ar: 3 g/s; Steam 3.4 g/s.	P(H_2O) = 0.4 bar; P(total) = 2 bar.	N/A	Integral
Phébus FPT3 [44]	B_4C control rod	~ 2100 ºC	Steam: ~ 0.5 g/s	P(total) = 2 bar.	N/A	Integral

* COLOSS includes both separate effects tests and integral tests, which are performed in the VERDI, TG and BOX rigs for B_4C oxidation, in QUENCH-SR rig for B_4C control rod degradation, and in CODEX- B_4C, QUENCH-07 and -09 for large-scale experiments.

4.2 Models recommended to THALES-2

All separate effects tests and integral tests can widely cover the temperature range supposed in severe accidents. It is recommended to select appropriate models for the eutectic interaction between B_4C and other materials, and oxidation of B_4C. There are no appropriate numerical models for the oxidation of B_4C-bearing mixtures, and all the corresponding conclusions describe reactions qualitatively. Thus, for the simplest consideration, the oxidation of B_4C-bearing mixtures will not be considered.

(1) Since the experiments performed by Nagase et al. cover the possible temperature range of a severe accident, the Nagase's correlations are recommended to model the eutectic interaction between B_4C and other materials. In order to evaluate the model uncertainty in eutectic interaction, Belovsky's correlation can be an option for comparison.

(2) Since the IRSN correlation includes the most complete experimental information, it is recommended to be used to model the oxidation of pure B_4C.

(3) The reaction fractions of all possible B_4C oxidation reactions, which are listed in Equation (14) ~ (16), can be decided by the simple or the advanced model applied in MELCOR 1.8.5. If methane generation rate is important and reducing atmospheres (high hydrogen concentrations) are expected, the advanced model in MELCOR 1.8.5 would be recommended. However, according to the literature review, the low production of methane by the B_4C oxidation process has been proven by several experiments.

5 Conclusions

The previous experiments and numerical modeling of the degradation of B_4C control rod have been investigated in this report. Investigated severe accidents codes include ATHLET-CD, ICARE2, SCDAP/RELAP5, SVECHA/QUENCH, MELCOR, MAAP and ASTEC. All of the interested questions described in Section 1 can be concluded. Mainly three essential parts of the B_4C degradation are reviewed.

(1) Eutectic interaction.

The eutectic interaction between B_4C and other materials will lower the melting point of components of control rods so that it will affect the early phase of core degradation. Significant melt formation occurs at temperature around 1250 ºC due to eutectic interactions between B_4C and surrounding stainless steel. The melting temperature is far below the melting point of each material.

(2) Oxidation of solid pure B_4C.

The modeling of pure B_4C oxidation is based on plenty of experiments performed worldwide. In severe accidents, B_4C oxidation starts from the failure of stainless steel tube. The formation of B_2O_3 layer outside of B_4C pellet is concluded as a parabolic rate function of temperature, but the consumption the B_2O_3 layer is a linear function of temperature. A parametric model of two equations is used to depict this phenomenon. IRSN B_4C oxidation kinetics is favored for including most of experimental data.

(3) Oxidation of B_4C-bearing mixture.

The oxidation of B_4C-bearing mixture is a more complicated phenomenon. The mathematical modeling is always of large uncertainty since sufficient technical knowledge has not been obtained. Qualitative experimental results are compared, but no quantitative kinetics is determined in current severe accident codes.

Reaction correlations of B_4C-related eutectic interaction and oxidation are compared and appropriate reaction correlations were recommended to be used in the severe accident modeling by THALES-2. However, the mechanistic modeling of B_4C-bearing mixture will not be included in THALES-2 since the complicated process and limited influences. The model and parameter uncertainties of B_4C control rod degradation will be evaluated in future researches.

References

[1] de Luze O. Degradation and oxidation of B_4C control rod segments at high temperatures. A review and code interpretation of the BECARRE program. Nuclear Engineering and Design, vol.259, pp.150-165, 2013.

[2] Belovsky L., et al. Chemical interactions in B_4C-filled control rod segments above 1000 ºC under transient conditions. 5th International Conference on Nuclear Engineering (ICONE5), Nice, France (CD-ROM, no. 2184), 1997.

[3] Adroguer B., et al. Core loss during a severe accident (COLOSS). Nuclear Engineering and Design, vol.221, pp.55-76, 2003.

[4] Steinbrück M. Influence of boron carbide on core degradation during severe accidents in LWRs. Annals of Nuclear Energy, vol.64, pp.43-49, 2014.

[5] Hofmann P., et al. Reaction behavior of B_4C absorber material with stainless steel and Zircaloy in severe LWR accidents. KfK 4598, Kernforschungszentrum Karlsruhe GmbH, Karlsruhe, Germany, 1989.

[6] Hofmann P., et al. Chemical interactions between as-received and pre-oxidized Zircaloy-4 and stainless steel at high temperatures. KfK 5106, Kernforschungszentrum Karlsruhe GmbH, Karlsruhe, Germany, 1994.

[7] Gauntt R.O., et al. The DF-4 fuel damage experiment in ACRR with a BWR control blade and channel box. NUREG/CR-4671, SAND86-1443, Sandia National Laboratories, Albuqucrque, New Mexico, USA, 1989.

[8] Sepold L., et al. Behavior of BWR-type fuel elements with B_4C/steel absorber tested under severe fuel damage conditions in the CORA facility. FZKA 7447, Forschungszentrum Karlsruhe GmbH, Karlsruhe, Germany, 2009.

[9] Uetsuka H., et al. Research activities at JAERI on core material behavior under accident conditions. Proceedings of a Technical Committee Meeting: Behavior of LWR Core Materials under Accident Conditions, Dimitrovgrad, Russian Federation (IAEA-TECHDOC-921, pp.23-38), 1995.

[10] Nagase F., et al. B_4C/Zircaloy reaction at temperatures from 1173 K to 1953 K. Journal of Nuclear Science and Technology, vol.34, pp.367-374, 1997.

[11] Nagase F., et al. Chemical interactions between B_4C and stainless steel at high temperatures. Journal of Nuclear Materials, vol.245, pp.52-59, 1997.

[12] Veshchunov M.S., et al. Modeling of B_4C interactions with Zircaloy at high temperatures. Journal of Nuclear Materials, vol.210, pp.11-20, 1994.

[13] Veshchunov M.S., et al. Modeling of the interactions between B_4C and stainless steel at high temperatures. Journal of Nuclear Materials, vol.226, pp.72-91, 1995.

[14] Bertrand F., et al.. B_4C control rod oxidation during a severe accident in a PWR reactor, separate effect and integral tests analysis for modeling purpose with the ICARE/CATHARE code. The 10th International Topical Meeting on Nuclear Reactor Thermal Hydraulics (NURETH-10), Seoul, Korea

(CD-ROM, no.G00004), 2003.

[15] Steinbrück M. Degradation and oxidation of B_4C control rod segments at high temperatures. FZKA 6980, Forschungszentrum Karlsruhe GmbH, Karlsruhe, Germany, 2004.

[16] Steinbrück M. Degradation and oxidation of B_4C control rod segments at high temperatures. Journal of Nuclear Materials, vol.400, pp.138-150, 2010.

[17] de Luze O., et al. Early phase fuel degradation in Phébus FP: initiating phenomena of degradation in fuel bundle tests. Annals of Nuclear Energy, vol.61, pp.23-35, 2013.

[18] Barrachin, M., et al. Late phase fuel degradation in the Phébus FP tests. Annals of Nuclear Energy, vol.61, pp.36-53, 2013.

[19] Elrick R.M. Boron carbide – steam reactions with cesium hydroxide and cesium iodide at 1270 K in an Inconel 600 system. NUREG/CR-4963, SAND87-1491, Sandia National Laboratories, Albuqucrque, New Mexico, USA, 1987.

[20] Sato T., et al. Oxidation of non-oxide ceramics by water vapor at high temperatures, Journal of The Society of Materials Science, Japan, vol.37 (412), pp.77-82, 1988.

[21] Liljenzin J.O., et al. The influence of chemistry on core melt accidents. Final report of the NKA project AKTI-150, Nordic Liaison Committee for Atomic Energy, 1990.

[22] Belovsky L. Heat release from B_4C oxidation in steam and air. Proceedings of a Technical Committee Meeting: Behavior of LWR Core Materials under Accident Conditions, Dimitrovgrad, Russian Federation (IAEA-TECHDOC-921, pp. 49-61), 1995.

[23] Adroguer B., et al. Core loss during a severe accident (COLOSS). Nuclear Engineering and Design, vol.235, pp.173-198, 2005.

[24] Steinbrück M. Oxidation of boron carbide at high temperatures. Journal of Nuclear Materials, vol.336, pp.185-193, 2005.

[25] Steiner H. Modeling of boron carbide oxidation in steam. Journal of Nuclear materials, vol.345, pp.75-83, 2005.

[26] Steinbrück M. Oxidation of B_4C by steam at high temperatures: new experiments and modeling. Nuclear Engineering and Design, vol.237, pp.161-181, 2007.

[27] Seiler N., et al. Investigation on boron carbide oxidation for nuclear reactors safety – general modeling for ICARE/CATHARE code applications. Nuclear Engineering and Design, vol.238, pp.820-836, 2008.

[28] Dominguez C., et al. Investigation on boron carbide oxidation for nuclear reactor safety: experiments in highly oxidizing conditions. Journal of Nuclear Materials, vol.374, pp.473-481, 2008.

[29] Repetto G., et al. B_4C oxidation modeling in severe accident codes: applications to PHEBUS and QUENCH experiments. Progress in Nuclear Energy, vol.52, pp.37-45, 2010.

[30] Haste T., et al. Study of boron behavior in the primary circuit of water reactors under severe accident conditions: a comparison of Phébus FPT3 results with other resent integral and separate-effects data. Nuclear Engineering and Design, vol.246, pp.147-156, 2012.

[31] Dominguez C. Steam oxidation of boron carbide-stainless steel liquid mixtures. Journal of Nuclear

Materials, vol.427, pp.140-151, 2012.

[32] Austregesilo H., et al. Post-test calculation and uncertainty analysis of the experiment QUENCH-07 with the system code ATHLET-CD. Nuclear Engineering and Design, vol.237, pp.1693-1703, 2007.

[33] Gauntt R.O., et al. MELCOR computer code manuals. NUREG/CR-6119, Vol. 1 & 2, Rev.2, SAND2000-2417/1, Sandia National Laboratories, Albuqucrque, New Mexico, USA, 2000.

[34] Chatelard P., et al. Assessment of ICARE/CATHARE V1 severe accident code. 14th International Conference on Nuclear Engineering (ICONE14), Miami, Florida, USA (CD-ROM, No.89307), 2006.

[35] Ederli S., et al. Oxidation of a B_4C control rod by steam. Implementation of a preliminary model in the ICARE2 code. Report D24, WP7.1, COLOSS project, 2001.

[36] Gauntt R.O., et al. MELCOR computer code manuals. NUREG/CR-6119. Vol.1 & 2, Rev.3. SAND2005-5713, Sandia National Laboratories, Albuqucrque, New Mexico, USA, 2005.

[37] Veshchunov M.S., et al. Modeling of B_4C oxidation by steam at high temperatures based on separate-effects tests and its application to the bundle experiment QUENCH-07. FZKA 7118, Forschungszentrum Karlsruhe GmbH, Karlsruhe, Germany, 2005.

[38] Steinbrück M. Experiments on the oxidation of boron carbide at high temperatures. FZKA 6979, Forschungszentrum Karlsruhe GmbH, Karlsruhe, Germany, 2004.

[39] Krauss W., et al. TG-rig tests (thermal balance) on the oxidation of B_4C. FZKA 6883, Forschungszentrum Karlsruhe GmbH, Karlsruhe, Germany, 2003.

[40] Hagen S., et al. Impact of absorber rod material on bundle degradation seen in CORA experiments. FZKA 5680, Forschungszentrum Karlsruhe GmbH, Karlsruhe, Germany, 1996.

[41] Steinbrück M., et al. Results of the B_4C control rod test QUENCH-07. FZKA 6746, Forschungszentrum Karlsruhe GmbH, Karlsruhe, Germany, 2004.

[42] Homann C., et al. Analysis and comparison of experimental data of bundle tests QUENCH-07 to QUENCH-09 about B_4C control rod behavior. FZKA 7101, Forschungszentrum Karlsruhe GmbH, Karlsruhe, Germany, 2006.

[43] Steinbrück M., et al. Results of the QUENCH-09 experiment with a B_4C control rod. FZKA 6829, Forschungszentrum Karlsruhe GmbH, Karlsruhe, Germany, 2004.

[44] Haste T., et al. Phébus FPT3: overview of main results concerning the behavior of fission products and structural materials in the containment. Nuclear Engineering and Design, vol.261, pp.333-345, 2013.

国際単位系（SI）

表１．SI 基本単位

基本量	SI 基本単位	
	名称	記号
長さ	メートル	m
質量	キログラム	kg
時間	秒	s
電流	アンペア	A
熱力学温度	ケルビン	K
物質量	モル	mol
光度	カンデラ	cd

表２．基本単位を用いて表されるSI組立単位の例

組立量	SI 基本単位	
	名称	記号
面積	平方メートル	m^2
体積	立法メートル	m^3
速さ，速度	メートル毎秒	m/s
加速度	メートル毎秒毎秒	m/s^2
波数	毎メートル	m^{-1}
密度，質量密度	キログラム毎立方メートル	kg/m^3
面積密度	キログラム毎平方メートル	kg/m^2
比体積	立方メートル毎キログラム	m^3/kg
電流密度	アンペア毎平方メートル	A/m^2
磁界の強さ	アンペア毎メートル	A/m
量濃度(a)，濃度	モル毎立方メートル	mol/m^3
質量濃度	キログラム毎立法メートル	kg/m^3
輝度	カンデラ毎平方メートル	cd/m^2
屈折率(b)	（数字の）　1	1
比透磁率(b)	（数字の）　1	1

(a) 量濃度（amount concentration）は臨床化学の分野では物質濃度（substance concentration）ともよばれる。
(b) これらは無次元量あるいは次元１をもつ量であるが、そのことを表す単位記号である数字の１は通常は表記しない。

表３．固有の名称と記号で表されるSI組立単位

組立量	SI 組立単位			
	名称	記号	他のSI単位による表し方	SI基本単位による表し方
平面角	ラジアン(b)	rad	1 (b)	m/m
立体角	ステラジアン(b)	sr$^{(c)}$	1 (b)	m$^{2/}$m^2
周波数	ヘルツ(d)	Hz		s^{-1}
力	ニュートン	N		m kg s^{-2}
圧力，応力	パスカル	Pa	N/m^2	m^{-1} kg s^{-2}
エネルギー，仕事，熱量	ジュール	J	N m	m^2 kg s^{-2}
仕事率，工率，放射束	ワット	W	J/s	m^2 kg s^{-3}
電荷，電気量	クーロン	C		s A
電位差（電圧），起電力	ボルト	V	W/A	m^2 kg s^{-3} A^{-1}
静電容量	ファラド	F	C/V	m^{-2} kg^{-1} s^4 A^2
電気抵抗	オーム	Ω	V/A	m^2 kg s^{-3} A^{-2}
コンダクタンス	ジーメンス	S	A/V	m^{-2} kg^{-1} s^3 A^2
磁束	ウエーバ	Wb	Vs	m^2 kg s^{-2} A^{-1}
磁束密度	テスラ	T	Wb/m^2	kg s^{-2} A^{-1}
インダクタンス	ヘンリー	H	Wb/A	m^2 kg s^{-2} A^{-2}
セルシウス温度	セルシウス度(e)	℃		K
光束	ルーメン	lm	cd sr$^{(c)}$	cd
照度	ルクス	lx	lm/m^2	m^{-2} cd
放射性核種の放射能(f)	ベクレル(d)	Bq		s^{-1}
吸収線量, 比エネルギー分与, カーマ	グレイ	Gy	J/kg	m^2 s^{-2}
線量当量, 周辺線量当量, 方向性線量当量, 個人線量当量	シーベルト(g)	Sv	J/kg	m^2 s^{-2}
酸素活性	カタール	kat		s^{-1} mol

(a)SI接頭語は固有の名称と記号を持つ組立単位と組み合わせても使用できる。しかし接頭語を付した単位はもはやコヒーレントではない。
(b)ラジアンとステラジアンは数字の１に対する単位の特別な名称で、量についての情報をつたえるために使われる。実際には、使用する時には記号rad及びsrが用いられるが、習慣として組立単位としての記号である数字の１は明示されない。
(c)測光学ではステラジアンという名称と記号srを単位の表し方の中に、そのまま維持している。
(d)ヘルツは周期現象についてのみ、ベクレルは放射性核種の統計的過程についてのみ使用される。
(e)セルシウス度はケルビンの特別な名称で、セルシウス温度を表すために使用される。セルシウス度とケルビンの単位の大きさは同一である。したがって、温度差や温度間隔を表す数値はどちらの単位で表しても同じである。
(f)放射性核種の放射能（activity referred to a radionuclide）は、しばしば誤った用語で”radioactivity”と記される。
(g)単位シーベルト（PV,2002,70,205）についてはCIPM勧告2（CI-2002）を参照。

表４．単位の中に固有の名称と記号を含むSI組立単位の例

組立量	SI 組立単位		
	名称	記号	SI 基本単位による表し方
粘度	パスカル秒	Pa s	m^{-1} kg s^{-1}
力のモーメント	ニュートンメートル	N m	m^2 kg s^{-2}
表面張力	ニュートン毎メートル	N/m	kg s^{-2}
角速度	ラジアン毎秒	rad/s	m m^{-1} s^{-1}=s^{-1}
角加速度	ラジアン毎秒毎秒	rad/s^2	m m^{-1} s^{-2}=s^{-2}
熱流密度，放射照度	ワット毎平方メートル	W/m^2	kg s^{-3}
熱容量，エントロピー	ジュール毎ケルビン	J/K	m^2 kg s^{-2} K^{-1}
比熱容量，比エントロピー	ジュール毎キログラム毎ケルビン	J/(kg K)	m^2 s^{-2} K^{-1}
比エネルギー	ジュール毎キログラム	J/kg	m^2 s^{-2}
熱伝導率	ワット毎メートル毎ケルビン	W/(m K)	m kg s^{-3} K^{-1}
体積エネルギー	ジュール毎立方メートル	J/m^3	m^{-1} kg s^{-2}
電界の強さ	ボルト毎メートル	V/m	m kg s^{-3} A^{-1}
電荷密度	クーロン毎立方メートル	C/m^3	m^{-3} sA
表面電荷	クーロン毎平方メートル	C/m^2	m^{-2} sA
電束密度，電気変位	クーロン毎平方メートル	C/m^2	m^{-2} sA
誘電率	ファラド毎メートル	F/m	m^{-3} kg^{-1} s^4 A^2
透磁率	ヘンリー毎メートル	H/m	m kg s^{-2} A^{-2}
モルエネルギー	ジュール毎モル	J/mol	m^2 kg s^{-2} mol^{-1}
モルエントロピー, モル熱容量	ジュール毎モル毎ケルビン	J/(mol K)	m^2 kg s^{-2} K^{-1} mol^{-1}
照射線量（X線及びγ線）	クーロン毎キログラム	C/kg	kg^{-1} sA
吸収線量率	グレイ毎秒	Gy/s	m^2 s^{-3}
放射強度	ワット毎ステラジアン	W/sr	m^4 m^{-2} kg s^{-3}=m^2 kg s^{-3}
放射輝度	ワット毎平方メートル毎ステラジアン	W/(m^2 sr)	m^2 m^{-2} kg s^{-3}=kg s^{-3}
酵素活性濃度	カタール毎立方メートル	kat/m^3	m^{-3} s^{-1} mol

表５．SI 接頭語

乗数	接頭語	記号	乗数	接頭語	記号
10^{24}	ヨタ	Y	10^{-1}	デシ	d
10^{21}	ゼタ	Z	10^{-2}	センチ	c
10^{18}	エクサ	E	10^{-3}	ミリ	m
10^{15}	ペタ	P	10^{-6}	マイクロ	µ
10^{12}	テラ	T	10^{-9}	ナノ	n
10^9	ギガ	G	10^{-12}	ピコ	p
10^6	メガ	M	10^{-15}	フェムト	f
10^3	キロ	k	10^{-18}	アト	a
10^2	ヘクト	h	10^{-21}	ゼプト	z
10^1	デカ	da	10^{-24}	ヨクト	y

表６．SIに属さないが、SIと併用される単位

名称	記号	SI 単位による値
分	min	1 min=60s
時	h	1h =60 min=3600 s
日	d	1 d=24 h=86 400 s
度	°	1°=(π/180) rad
分	’	1’=(1/60)°=(π/10800) rad
秒	”	1”=(1/60)’=(π/648000) rad
ヘクタール	ha	1ha=1hm^2=10^{4}m^2
リットル	L，l	1L=1l=1dm^3=10^{3}cm^3=10^{-3}m^3
トン	t	1t=10^3 kg

表７．SIに属さないが、SIと併用される単位で、SI単位で表される数値が実験的に得られるもの

名称	記号	SI 単位で表される数値
電子ボルト	eV	1eV=1.602 176 53(14)×10^{-19}J
ダルトン	Da	1Da=1.660 538 86(28)×10^{-27}kg
統一原子質量単位	u	1u=1 Da
天文単位	ua	1ua=1.495 978 706 91(6)×10^{11}m

表８．SIに属さないが、SIと併用されるその他の単位

名称	記号	SI 単位で表される数値
バール	bar	1 bar=0.1MPa=100kPa=10^{5}Pa
水銀柱ミリメートル	mmHg	1mmHg=133.322Pa
オングストローム	Å	1 Å=0.1nm=100pm=10^{-10}m
海里	M	1 M=1852m
バーン	b	1 b=100fm^2=(10^{-12}cm)2=10^{-28}m^2
ノット	kn	1 kn=(1852/3600)m/s
ネーパ	Np	SI単位との数値的な関係は、対数量の定義に依存。
ベル	B	
デジベル	dB	

表９．固有の名称をもつCGS組立単位

名称	記号	SI 単位で表される数値
エルグ	erg	1 erg=10^{-7} J
ダイン	dyn	1 dyn=10^{-5}N
ポアズ	P	1 P=1 dyn s cm^{-2}=0.1Pa s
ストークス	St	1 St =1cm^2 s^{-1}=10^{-4}m^2 s^{-1}
スチルブ	sb	1 sb =1cd cm^{-2}=10^{4}cd m^{-2}
フォト	ph	1 ph=1cd sr cm^{-2} 10^{4}lx
ガル	Gal	1 Gal =1cm s^{-2}=10^{-2}ms^{-2}
マクスウェル	Mx	1 Mx = 1G cm^2=10^{-8}Wb
ガウス	G	1 G =1Mx cm^{-2} =10^{-4}T
エルステッド(c)	Oe	1 Oe ≙ (10^3/4π)A m^{-1}

(c) ３元系のCGS単位系とSIでは直接比較できないため、等号「 ≙ 」は対応関係を示すものである。

表10．SIに属さないその他の単位の例

名称	記号	SI 単位で表される数値
キュリー	Ci	1 Ci=3.7×10^{10}Bq
レントゲン	R	1 R = 2.58×10^{-4}C/kg
ラド	rad	1 rad=1cGy=10^{-2}Gy
レム	rem	1 rem=1 cSv=10^{-2}Sv
ガンマ	γ	1 γ =1 nT=10-9T
フェルミ		1フェルミ=1 fm=10-15m
メートル系カラット		1メートル系カラット = 200 mg = 2×10-4kg
トル	Torr	1 Torr = (101 325/760) Pa
標準大気圧	atm	1 atm = 101 325 Pa
カロリー	cal	1cal=4.1858J（「15℃」カロリー），4.1868J（「IT」カロリー）4.184J（「熱化学」カロリー）
ミクロン	µ	1 µ =1µm=10^{-6}m

（第8版，2006年改訂）